18.S096: Graphs, Diffusion Maps, and Semi-supervised Learning

Topics in Mathematics of Data Science (Fall 2015)

Afonso S. Bandeira

bandeira@mit.edu

http://math.mit.edu/~bandeira

September 30, 2015

These are lecture notes not in final form and will be continuously edited and/or corrected (as I am sure it contains many typos). Please let me know if you find any typo/mistake. Also, I am posting short descriptions of these notes (together with the open problems) on my Blog, see [Ban15].

2.1 Graphs

Graphs will be one of the main objects of study through these lectures, it is time to introduce them. A graph $G = (V, E)$ contains a set of nodes $V = \{v_1, \ldots, v_n\}$ and edges $E \subseteq \binom{V}{2}$. An edge $(i, j) \in E$ if v_i and v_j are connected. Here is one of the graph theorists favorite examples, the Petersen graph[1]:
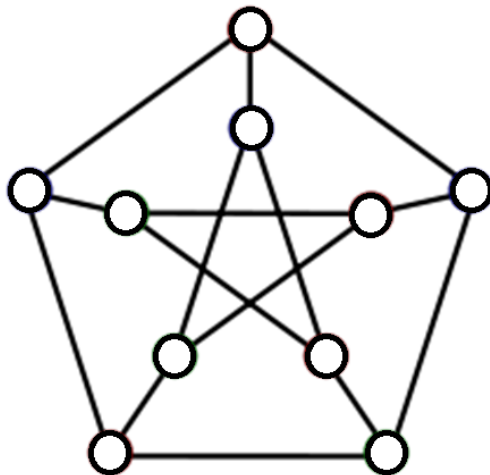

Figure 1: The Petersen graph

Graphs are crucial tools in many fields, the intuitive reason being that many phenomena, while complex, can often be thought about through pairwise interactions between objects (or data points),

---

[1]The Peterson graph is often used as a counter-example in graph theory.

which can be nicely modeled with the help of a graph.

Let us recall some concepts about graphs that we will need.

- A graph is connected if, for all pairs of vertices, there is a path between these vertices on the graph. The number of connected components is simply the size of the smallest partition of the nodes into connected subgraphs. The Petersen graph is connected (and thus it has only 1 connected component).

- A clique of a graph G is a subset S of its nodes such that the subgraph corresponding to it is complete. In other words S is a clique if all pairs of vertices in S share an edge. The clique number $c(G)$ of G is the size of the largest clique of G. The Petersen graph has a clique number of 2.

- An independence set of a graph G is a subset S of its nodes such that no two nodes in S share an edge. Equivalently it is a clique of the complement graph $G^c := (V, E^c)$. The independence number of G is simply the clique number of S^c. The Petersen graph has an independence number of 4.

A particularly useful way to represent a graph is through its adjacency matrix. Given a graph $G = (V, E)$ on n nodes ($|V| = n$), we define its adjacency matrix $A \in \mathbb{R}^{n \times n}$ as the symmetric matrix with entries

$$A_{ij} = \begin{cases} 1 & \text{if } (i, j) \in E, \\ 0 & \text{otherwise.} \end{cases}$$

Sometime, we will consider weighted graphs $G = (V, E, W)$, where edges may have weights w_{ij}, we think of the weights as non-negative $w_{ij} \geq 0$ and symmetric $w_{ij} = w_{ji}$.

2.1.1 Cliques and Ramsey numbers

Cliques are important structures in graphs and may have important application-specific applications. For example, in a social network graph (e.g., where people correspond to vertices and two vertices are connected if the respective people are friends) cliques have a clear interpretation.

A natural question is whether it is possible to have arbitrarily large graphs without cliques (and without it's complement having cliques), Ramsey answer this question in the negative in 1928 [Ram28]. Let us start with some definitions: given a graph G we define $r(G)$ as the size of the largest clique of independence set, i.e.

$$r(G) := \max \{ c(G), c(G^c) \}.$$

Given r, let $R(r)$ denote the smallest integer n such that every graph G on n nodes must have $r(G) \geq r$. Ramsey [Ram28] showed that $R(r)$ is finite, for every r.

Remark 2.1 *It is easy to show that $R(3) \leq 6$, try it!*

We will need a simple estimate for what follows (it is a very useful consequence of Stirling's approximation, e.g.).

Proposition 2.2 *For every $k \leq n$ positive integers,*

$$\left(\frac{n}{k}\right)^k \leq \binom{n}{r} \leq \left(\frac{ne}{k}\right)^k.$$

We will show a simple lower bound on $R(r)$. But first we introduce a random graph construction, an Erdős-Renyí graph.

Definition 2.3 *Given n and p, the random Erdős-Renyí graph $G(n,p)$ is a random graph on n vertices where each possible edge appears, independently, with probability p.*

The proof of the lower bound on $R(r)$ is based on the probabilistic method, a beautiful non-constructive method pioneered by Paul Erdős to establish the existence of certain objects. The core idea is the simple observation that if a random variable has a certain expectation then there must exist a draw of it whose value is at least that of the expectation. It is best understood with an example.

Theorem 2.4 *For every $r \geq 2$,*

$$R(r) \geq 2^{\frac{r-1}{2}}.$$

Proof. Let G be drawn from the $G\left(n, \frac{1}{2}\right)$ distribution, $G \sim G\left(n, \frac{1}{2}\right)$. For every set S of r nodes, let $X(S)$ denote the random variable

$$X(S) = \begin{cases} 1 & \text{if } S \text{ is a clique or independent set,} \\ 0 & \text{otherwise.} \end{cases}$$

Also, let X denote the random variable

$$X = \sum_{S \in \binom{V}{r}} X(S).$$

We will proceed by estimating $\mathbb{E}[X]$. Note that, by linearity of expectation,

$$\mathbb{E}[X] = \sum_{S \in \binom{V}{r}} \mathbb{E}[X(S)],$$

and $\mathbb{E}[X(S)] = \text{Prob}\{S \text{ is a clique or independent set}\} = \frac{2}{2^{\binom{|S|}{2}}}$. This means that

$$\mathbb{E}[X] = \sum_{S \in \binom{V}{r}} \frac{2}{2^{\binom{|S|}{2}}} = \binom{n}{r} \frac{2}{2^{\binom{r}{2}}} = \binom{n}{r} \frac{2}{2^{\frac{r(r-1)}{2}}}.$$

By Proposition 2.2 we have,

$$\mathbb{E}[X] \leq \left(\frac{ne}{r}\right)^r \frac{2}{2^{\frac{r(r-1)}{2}}} = 2\left(\frac{n}{2^{\frac{r-1}{2}}} \frac{e}{r}\right)^r.$$

That means that if $n \leq 2^{\frac{r-1}{2}}$ and $r \geq 3$ then $\mathbb{E}[X] < 1$. This means that $\text{Prob}\{X < 1\} > 0$ and since X is a non-negative integer we must have $\text{Prob}\{X = 0\} = \text{Prob}\{X < 1\} > 0$ (another way of saying

that is that if $\mathbb{E}[X] < 1$ then there must be an instance for which $X < 1$ and since X is a non-negative integer, we must have $X = 0$). This means that there exists a graph with $2^{\frac{r-1}{2}}$ nodes that does not have cliques or independent sets of size r which implies the theorem. $\qquad\square$

Remarkably, this lower bound is not very different from the best known. In fact, the best known lower and upper bounds known [Spe75, Con09] for $R(r)$ are

$$(1 + o(1))\frac{\sqrt{2}r}{e}\left(\sqrt{2}\right)^r \le R(r) \le r^{-\frac{c\log r}{\log\log r}}4^r. \tag{1}$$

Open Problem 2.1 *Recall the definition of $R(r)$ above, the following questions are open:*

- *What is the value of $R(5)$?*

- *What are the asymptotics of $R(s)$? In particular, improve on the base of the exponent on either the lower bound ($\sqrt{2}$) or the upper bound (4).*

- *Construct a family of graphs $G = (V, E)$ with increasing number of vertices for which there exists $\varepsilon > 0$ such that[2]*
$$|V| \lesssim (1 + \varepsilon)^r.$$

It is known that $43 \le R(5) \le 49$. There is a famous quote in Joel Spencer's book [Spe94] that conveys the difficulty of computing Ramsey numbers:

"Erdős asks us to imagine an alien force, vastly more powerful than us, landing on Earth and demanding the value of $R(5)$ or they will destroy our planet. In that case, he claims, we should marshal all our computers and all our mathematicians and attempt to find the value. But suppose, instead, that they ask for $R(6)$. In that case, he believes, we should attempt to destroy the aliens."

There is an alternative useful way to think about 1, by taking $\log_2$ of each bound and rearranging, we get that

$$\left(\frac{1}{2} + o(1)\right)\log_2 n \le \min_{G=(V,E),\, |V|=n} r(G) \le (2 + o(1))\log_2 n$$

The current "world record" (see [CZ15, Coh15]) for deterministic construction of families of graphs with small $r(G)$ achieves $r(G) \lesssim 2^{(\log\log|V|)^c}$, for some constant $c > 0$. Note that this is still considerably larger than polylog $|V|$. In contrast, it is very easy for randomized constructions to satisfy $r(G) \le 2\log_2 n$, as made precise by the folloing theorem.

Theorem 2.5 *Let $G \sim G\left(n, \frac{1}{2}\right)$ be and Erdős-Renyí graph with edge probability $\frac{1}{2}$. Then, with high probability,[3]*
$$R(G) \le 2\log_2(n).$$

---

[2]By $a_k \lesssim b_k$ we mean that there exists a constant c such that $a_k \le c\, b_k$.
[3]We say an event happens with high probability if its probability is $\ge 1 - n^{-\Omega(1)}$.

Proof. Given n, we are interested in upper bounding $\text{Prob}\left\{R(G) \geq \lceil 2\log_2 n \rceil\right\}$. and we proceed by union bounding (and making use of Proposition 2.2):

$$
\begin{aligned}
\text{Prob}\left\{R(G) \geq \lceil 2\log_2 n \rceil\right\} &= \text{Prob}\left\{\exists_{S \subset V, |S| = \lceil 2\log_2 n \rceil} \ S \text{ is a clique or independent set}\right\} \\
&= \text{Prob}\left\{\bigcup_{S \in \binom{V}{\lceil 2\log_2 n \rceil}} \{S \text{ is a clique or independent set}\}\right\} \\
&\leq \sum_{S \in \binom{V}{\lceil 2\log_2 n \rceil}} \text{Prob}\left\{S \text{ is a clique or independent set}\right\} \\
&= \binom{n}{\lceil 2\log_2 n \rceil} \frac{2}{2^{\binom{\lceil 2\log_2 n \rceil}{2}}} \\
&\leq 2\left(\frac{n}{2^{\frac{\lceil 2\log_2 n \rceil - 1}{2}}} \frac{e}{\lceil 2\log_2 n \rceil}\right)^{\lceil 2\log_2 n \rceil} \\
&\leq 2\left(\frac{e\sqrt{2}}{2\log_2 n}\right)^{\lceil 2\log_2 n \rceil} \\
&\lesssim n^{-\Omega(1)}.
\end{aligned}
$$

$\square$

The following is one of the most fascinating conjectures in Graph Theory

Open Problem 2.2 (Erdős-Hajnal Conjecture [EH89]) *Prove or disprove the following:*

For any finite graph H, there exists a constant $\delta_H > 0$ such that any graph on n nodes that does not contain H as a subgraph (is a H-free graph) must have

$$ r(G) \gtrsim n^{\delta_H}. $$

It is known that $r(G) \gtrsim \exp\left(c_H\sqrt{\log n}\right)$, for some constant $c_H > 0$ (see [Chu13] for a survey on this conjecture). Note that this lower bound already shows that H-free graphs need to have considerably larger $r(G)$. This is an amazing local to global effect, where imposing a constraint on small groups of vertices are connected (being H-free is a local property) creates extremely large cliques or independence sets (much larger than $\text{polylog}(n)$ as in random Erdős-Renyí graphs).

Since we do not know how to deterministically construct graphs with $r(G) \leq \text{polylog } n$, one approach could be to take $G \sim G\left(n, \frac{1}{2}\right)$ and check that indeed it has small clique and independence number. However, finding the largest clique on a graph is known to be NP-hard (meaning that there is no polynomial time algorithm to solve it, provided that the widely believed conjecture $NP \neq P$ holds). That is a worst-case statement and thus it doesn't necessarily mean that it is difficult to find the clique number of random graphs. That being said, the next open problem suggests that this is indeed still difficult.

First let us describe a useful construct. Given n and ω, let us consider a random graph G that consists of taking a graph drawn from $G\left(n, \frac{1}{2}\right)$, picking ω of its nodes (say at random) and adding an

edge between every pair of those ω nodes, thus "planting" a clique of size ω. This will create a clique of size ω in G. If $\omega > 2\log_2 n$ this clique is larger than any other clique that was in the graph before planting. This means that, if $\omega > 2\log_2 n$, there is enough information in the graph to find the planted clique. In fact, one can simply look at all subsets of size $2\log_2 n + 1$ and check wether it is clique: if it is a clique then it very likely these vertices belong to the planted clique. However, checking all such subgraphs takes super-polynomial time $\sim n^{\mathcal{O}(\log n)}$. This motivates the natural question of whether this can be done in polynomial time.

Since the degrees of the nodes of a $G\left(n, \frac{1}{2}\right)$ have expected value $\frac{n-1}{2}$ and standard deviation $\sim \sqrt{n}$, if $\omega > c\sqrt{n}$ (for sufficiently large constant c) then the degrees of the nodes involved in the planted clique will have larger degrees and it is easy to detect (and find) the planted clique. Remarkably, there is no known method to work for ω significant smaller than this. There is a quasi-linear time algorithm [DM13] that finds the largest clique, with high probability, as long as $\omega \geq \sqrt{\frac{n}{e}} + o(\sqrt{n})$.[4]

Open Problem 2.3 (The planted clique problem) *Let G be a random graph constructed by taking a $G\left(n, \frac{1}{2}\right)$ and planting a clique of size ω.*

1. *Is there a polynomial time algorithm that is able to find the largest clique of G (with high probability) for $\omega \ll \sqrt{n}$. For example, for $\omega \approx \frac{\sqrt{n}}{\log n}$.*

2. *Is there a polynomial time algorithm that is able to distinguish, with high probability, G from a draw of $G\left(n, \frac{1}{2}\right)$ for $\omega \ll \sqrt{n}$. For example, for $\omega \approx \frac{\sqrt{n}}{\log n}$.*

3. *Is there a quasi-linear time algorithm able to find the largest clique of G (with high probability) for $\omega \leq \left(\frac{1}{\sqrt{e}} - \varepsilon\right)\sqrt{n}$, for some $\varepsilon > 0$.*

This open problem is particularly important. In fact, the hypothesis that finding planted cliques for small values of ω is behind several cryptographic protocols, and hardness results in average case complexity (hardness for Sparse PCA being a great example [BR13]).

2.2 Diffusion Maps

Diffusion Maps will allows us to represent (weighted) graphs $G = (V, E, W)$ in $\mathbb{R}^d$, i.e. associating, to each node, a point in $\mathbb{R}^d$. As we will see below, oftentimes when we have a set of data points $x_1, \ldots, x_n \in \mathbb{R}^p$ it will be beneficial to first associate to each a graph and then use Diffusion Maps to represent the points in d-dimensions, rather than using something like Principal Component Analysis.

Before presenting Diffusion Maps, we'll introduce a few important notions. Given $G = (V, E, W)$ we consider a random walk (with independent steps) on the vertices of V with transition probabilities:

$$\text{Prob}\left\{X(t+1) = j | X(t) = i\right\} = \frac{w_{ij}}{\deg(i)},$$

where $\deg(i) = \sum_j w_{ij}$. Let M be the matrix of these probabilities,

$$M_{ij} = \frac{w_{ij}}{\deg(i)}.$$

---

[4]There is an amplification technique that allows one to find the largest clique for $\omega \approx c\sqrt{n}$ for arbitrarily small c in polynomial time, where the exponent in the runtime depends on c. The rough idea is to consider all subsets of a certain finite size and checking whether the planted clique contains them.

It is easy to see that $M_{ij} \geq 0$ and $M\mathbf{1} = \mathbf{1}$ (indeed, M is a transition probability matrix). Defining D as the diagonal matrix with diagonal entries $D_{ii} = \deg(i)$ we have

$$M = D^{-1}W.$$

If we start a random walker at node i $(X(0) = 1)$ then the probability that, at step t, is at node j is given by

$$\text{Prob}\,\{X(t) = j | X(0) = i\} = \left(M^t\right)_{ij}.$$

In other words, the probability cloud of the random walker at point t, given that it started at node i is given by the row vector

$$\text{Prob}\,\{X(t) | X(0) = i\} = e_i^T M^t = M^t[i, :].$$

Remark 2.6 *A natural representation of the graph would be to associate each vertex to the probability cloud above, meaning*

$$i \to M^t[i, :].$$

This would place nodes i_1 and i_2 for which the random walkers starting at i_1 and i_2 have, after t steps, very similar distribution of locations. However, this would require $d = n$. In what follows we will construct a similar mapping but for considerably smaller d.

M is not symmetric, but a matrix similar to M, $S = D^{\frac{1}{2}}MD^{-\frac{1}{2}}$ is, indeed $S = D^{-\frac{1}{2}}WD^{-\frac{1}{2}}$. We consider the spectral decomposition of S

$$S = V\Lambda V^T,$$

where $V = [v_1, \ldots, v_n]$ satisfies $V^T V = I_{n \times n}$ and Λ is diagonal with diagonal elements $\Lambda_{kk} = \lambda_k$ (and we organize them as $\lambda_1 \geq \lambda_2 \geq \cdots \geq \lambda_n$). Note that $Sv_k = \lambda_k v_k$. Also,

$$M = D^{-\frac{1}{2}}SD^{\frac{1}{2}} = D^{-\frac{1}{2}}V\Lambda V^T D^{\frac{1}{2}} = \left(D^{-\frac{1}{2}}V\right) \Lambda \left(D^{\frac{1}{2}}V\right)^T.$$

We define $\Phi = D^{-\frac{1}{2}}V$ with columns $\Phi = [\varphi_1, \ldots, \varphi_n]$ and $\Psi = D^{\frac{1}{2}}V$ with columns $\Psi = [\psi_1, \ldots, \psi_n]$. Then

$$M = \Phi\Lambda\Psi^T,$$

and Φ, Ψ form a biorthogonal system in the sense that $\Phi^T \Psi = I_{n \times n}$ or, equivalently, $\varphi_j^T \psi_k = \delta_{jk}$. Note that φ_k and ψ_k are, respectively right and left eigenvectors of M, indeed, for all $1 \leq k \leq n$:

$$M\varphi_k = \lambda_k \varphi_k \quad \text{and } \psi_k^T M = \lambda_k \psi_k^T.$$

Also, we can rewrite this decomposition as

$$M = \sum_{k=1}^n \lambda_k \varphi_k \psi_k^T.$$

and it is easy to see that

$$M^t = \sum_{k=1}^n \lambda_k^t \varphi_k \psi_k^T. \tag{2}$$

Let's revisit the embedding suggested on Remark 2.6. It would correspond to

$$v_i \rightarrow M^t[i,:] = \sum_{k=1}^{n} \lambda_k^t \varphi_k(i) \psi_k^T,$$

it is written in terms of the basis ψ_k. The Diffusion Map will essentially consist of the representing a node i by the coefficients of the above map

$$v_i \rightarrow M^t[i,:] = \begin{bmatrix} \lambda_1^t \varphi_1(i) \\ \lambda_2^t \varphi_2(i) \\ \vdots \\ \lambda_n^t \varphi_n(i) \end{bmatrix}, \tag{3}$$

Note that $M\mathbf{1} = \mathbf{1}$, meaning that one of the right eigenvectors φ_k is simply a multiple of $\mathbf{1}$ and so it does not distinguish the different nodes of the graph. We will show that this indeed corresponds to the the first eigenvalue.

Proposition 2.7 *All eigenvalues λ_k of M satisfy $|\lambda_k| \leq 1$.*

Proof.
    Let φ_k be a right eigenvector associated with λ_k whose largest entry in magnitude is positive $\varphi_k(i_{\max})$. Then,

$$\lambda_k \varphi_k(i_{\max}) = M\varphi_k(i_{\max}) = \sum_{j=1}^{n} M_{i_{\max},j} \varphi_k(j).$$

This means, by triangular inequality that, that

$$|\lambda_k| = \sum_{j=1}^{n} |M_{i_{\max},j}| \frac{|\varphi_k(j)|}{|\varphi_k(i_{\max})|} \leq \sum_{j=1}^{n} |M_{i_{\max},j}| = 1.$$

$\square$

Remark 2.8 *It is possible that there are other eigenvalues with magnitude 1 but only if G is disconnected or if G is bipartite. Provided that G is disconnected, a natural way to remove potential periodicity issues (like the graph being bipartite) is to make the walk lazy, i.e. to add a certain probability of the walker to stay in the current node. This can be conveniently achieved by taking, e.g.,*

$$M' = \frac{1}{2}M + \frac{1}{2}I.$$

By the proposition above we can take $\varphi_1 = \mathbf{1}$, meaning that the first coordinate of (3) does not help differentiate points on the graph. This suggests removing that coordinate:

Definition 2.9 (Diffusion Map) *Given a graph $G = (V, E, W)$ construct M and its decomposition $M = \Phi\Lambda\Psi^T$ as described above. The Diffusion Map is a map $\phi_t : V \to \mathbb{R}^{n-1}$ given by*

$$\phi_t(v_i) = \begin{bmatrix} \lambda_2^t \varphi_2(i) \\ \lambda_3^t \varphi_3(i) \\ \vdots \\ \lambda_n^t \varphi_n(i) \end{bmatrix}.$$

This map is still a map to $n-1$ dimensions. But note now that each coordinate has a factor of λ_k^t which, if λ_k is small will be rather small for moderate values of t. This motivates truncating the Diffusion Map by taking only the first d coefficients.

Definition 2.10 (Truncated Diffusion Map) *Given a graph $G = (V, E, W)$ and dimension d, construct M and its decomposition $M = \Phi\Lambda\Psi^T$ as described above. The Diffusion Map truncated to d dimensions is a map $\phi_t : V \to \mathbb{R}^d$ given by*

$$\phi_t^{(d)}(v_i) = \begin{bmatrix} \lambda_2^t \varphi_2(i) \\ \lambda_3^t \varphi_3(i) \\ \vdots \\ \lambda_{d+1}^t \varphi_{d+1}(i) \end{bmatrix}.$$

In the following theorem we show that the euclidean distance in the diffusion map coordinates (called diffusion distance) meaningfully measures distance between the probability clouds after t iterations.

Theorem 2.11 *For any pair of nodes v_{i_1}, v_{i_2} we have*

$$\|\phi_t(v_{i_1}) - \phi_t(v_{i_2})\|^2 = \sum_{j=1}^{n} \frac{1}{\deg(j)} \left[\text{Prob}\{X(t) = j | X(0) = i_1\} - \text{Prob}\{X(t) = j | X(0) = i_2\} \right]^2.$$

Proof.

Note that $\sum_{j=1}^{n} \frac{1}{\deg(j)} \left[\text{Prob}\{X(t) = j | X(0) = i_1\} - \text{Prob}\{X(t) = j | X(0) = i_2\} \right]^2$ can be rewritten as

$$\sum_{j=1}^{n} \frac{1}{\deg(j)} \left[\sum_{k=1}^{n} \lambda_k^t \varphi_k(i_1) \psi_k(j) - \sum_{k=1}^{n} \lambda_k^t \varphi_k(i_2) \psi_k(j) \right]^2 = \sum_{j=1}^{n} \frac{1}{\deg(j)} \left[\sum_{k=1}^{n} \lambda_k^t \left(\varphi_k(i_1) - \varphi_k(i_2) \right) \psi_k(j) \right]^2$$

and

$$\sum_{j=1}^{n} \frac{1}{\deg(j)} \left[\sum_{k=1}^{n} \lambda_k^t \left(\varphi_k(i_1) - \varphi_k(i_2) \right) \psi_k(j) \right]^2 = \sum_{j=1}^{n} \left[\sum_{k=1}^{n} \lambda_k^t \left(\varphi_k(i_1) - \varphi_k(i_2) \right) \frac{\psi_k(j)}{\sqrt{\deg(j)}} \right]^2$$

$$= \left\| \sum_{k=1}^{n} \lambda_k^t \left(\varphi_k(i_1) - \varphi_k(i_2) \right) D^{-\frac{1}{2}} \psi_k \right\|^2.$$

9

Note that $D^{-\frac{1}{2}}\psi_k = v_k$ which forms an orthonormal basis, meaning that

$$\left\| \sum_{k=1}^{n} \lambda_k^t \left(\varphi_k(i_1) - \varphi_k(i_2) \right) D^{-\frac{1}{2}} \psi_k \right\|^2 = \sum_{k=1}^{n} \left(\lambda_k^t \left(\varphi_k(i_1) - \varphi_k(i_2) \right) \right)^2$$

$$= \sum_{k=2}^{n} \left(\lambda_k^t \varphi_k(i_1) - \lambda_k^t \varphi_k(i_2) \right)^2,$$

where the last inequality follows from the fact that $\varphi_1 = \mathbf{1}$ and concludes the proof of the theorem.
$\square$

2.2.1 A couple of examples

The ring graph is a graph on n nodes $\{1, \ldots, n\}$ such that node k is connected to $k-1$ and $k+1$ and 1 is connected to n. Figure 2 has the Diffusion Map of it truncated to two dimensions
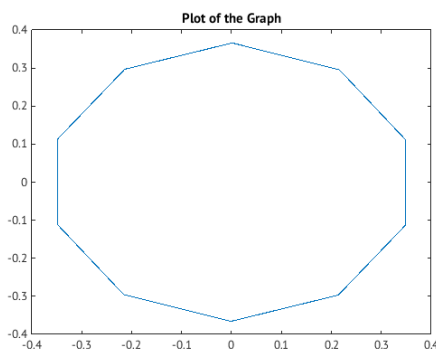
Figure 2: The Diffusion Map of the ring graph gives a very natural way of displaying (indeed, if one is asked to draw the ring graph, this is probably the drawing that most people would do). It is actually not difficult to analytically compute the Diffusion Map of this graph and confirm that it displays the points in a circle.

Another simple graph is K_n, the complete graph on n nodes (where every pair of nodes share an edge), see Figure 3.

2.2.2 Diffusion Maps of point clouds

Very often we are interested in embedding in $\mathbb{R}^d$ a point cloud of points $x_1, \ldots, x_n \in \mathbb{R}^p$ and necessarily a graph. One option (as discussed before in the course) is to use Principal Component Analysis (PCA), but PCA is only designed to find linear structure of the data and the low dimensionality of the dataset may be non-linear. For example, let's say our dataset is images of the face of someone taken from different angles and lighting conditions, for example, the dimensionality of this dataset is limited by the amount of muscles in the head and neck and by the degrees of freedom of the lighting conditions
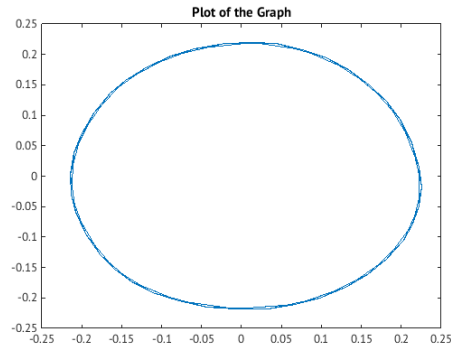
Figure 3: The Diffusion Map of the complete graph on 4 nodes in 3 dimensions appears to be a regular tetrahedron suggesting that there is no low dimensional structure in this graph. This is not surprising, since every pair of nodes is connected we don't expect this graph to have a natural representation in low dimensions.

(see Figure **??**) but it is not clear that this low dimensional structure is linearly apparent on the pixel values of the images.

Let's say that we are given a point cloud that is sampled from a two dimensional swiss roll embedded in three dimension (see Figure 4). In order to learn the two dimensional structure of this object we need to differentiate points that are near eachother because they are close by in the manifold and not simply because the manifold is curved and the points appear nearby even when they really are distant in the manifold (see Figure 4 for an example). We will achieve this by creating a graph from the data points.
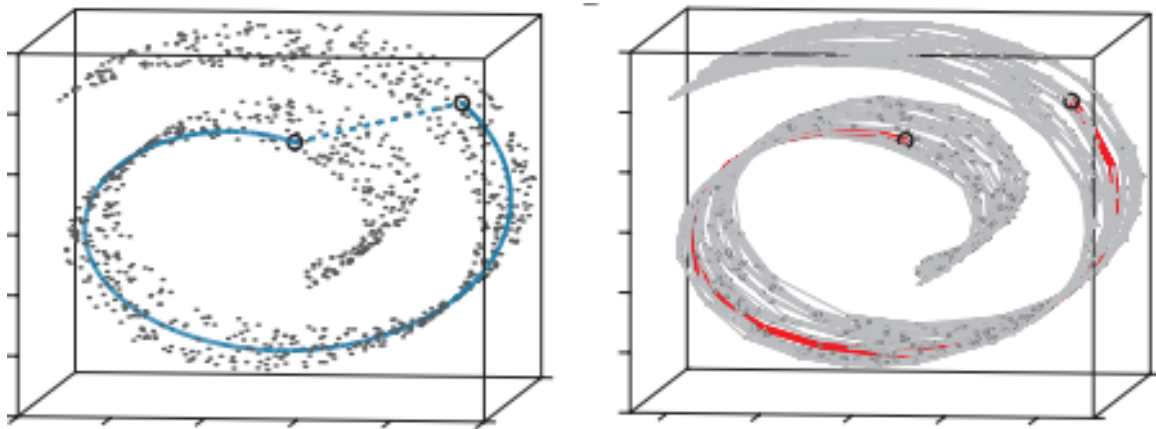
Figure 4: A swiss roll point cloud (see, for example, [TdSL00]). The points are sampled from a two dimensional manifold curved in $\mathbb{R}^3$ and then a graph is constructed where nodes correspond to points.

Our goal is for the graph to capture the structure of the manifold. To each data point we will

11

associate a node. For this we should only connect points that are close in the manifold and not points that maybe appear close in Euclidean space simply because of the curvature of the manifold. This is achieved by picking a small scale and linking nodes if they correspond to points whose distance is smaller than that scale. This is usually done smoothly via a kernel K_ε, and to each edge (i, j) associating a weight

$$w_{ij} = K_\varepsilon \left(\|x_i - x_j\|_2 \right),$$

a common example of a Kernel is $K_\varepsilon(u) = \exp\left(-\frac{1}{2\varepsilon} u^2\right)$, that gives essentially zero weight to edges corresponding to pairs of nodes for which $\|x_i - x_j\|_2 \gg \sqrt{\varepsilon}$. We can then take the the Diffusion Maps of the resulting graph.

2.2.3   A simple example

A simple and illustrative example is to take images of a blob on a background in different positions (image a white square on a black background and each data point corresponds to the same white square in different positions). This dataset is clearly intrinsically two dimensional, as each image can be described by the (two-dimensional) position of the square. However, we don't expect this two-dimensional structure to be directly apparent from the vectors of pixel values of each image; in particular we don't expect these vectors to lie in a two dimensional affine subspace!

Let's start by experimenting with the above example for one dimension. In that case the blob is a vertical stripe and simply moves left and right. We think of our space as the in the arcade game Asteroids, if the square or stripe moves to the right all the way to the end of the screen, it shows up on the left side (and same for up-down in the two-dimensional case). Not only this point cloud should have a one dimensional structure but it should also exhibit a circular structure. Remarkably, this structure is completely apparent when taking the two-dimensional Diffusion Map of this dataset, see Figure 5.
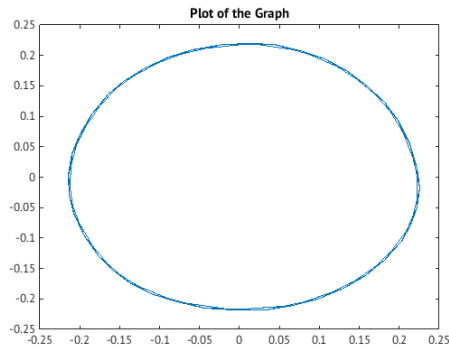

Figure 5: The two-dimensional diffusion map of the dataset of the datase where each data point is an image with the same vertical strip in different positions in the x-axis, the circular structure is apparent.

For the two dimensional example, we expect the structure of the underlying manifold to be a two-dimensional torus. Indeed, Figure 6 shows that the three-dimensional diffusion map captures the
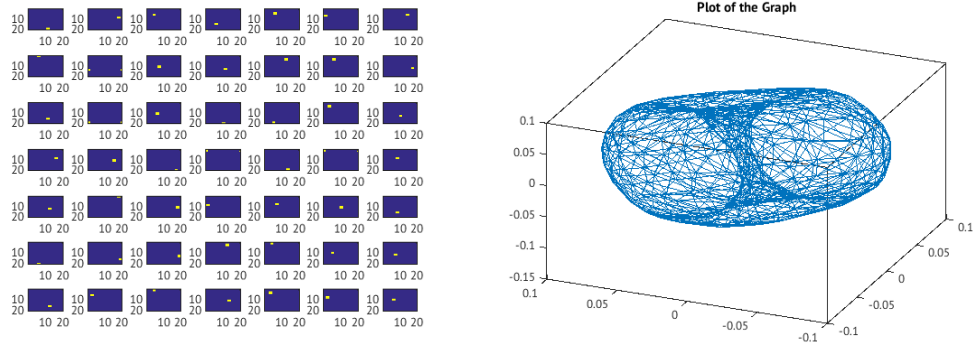
toroidal structure of the data.

Figure 6: On the left the data set considered and on the right its three dimensional diffusion map, the fact that the manifold is a torus is remarkably captured by the embedding.

2.2.4 Similar non-linear dimensional reduction techniques

There are several other similar non-linear dimensional reduction methods. A particularly popular one is ISOMAP [**?**]. The idea is to find an embedding in $\mathbb{R}_d$ for which euclidean distances in the embedding correspond as much as possible to geodesic distances in the graph. This can be achieved by, between pairs of nodes v_i, v_j finding their geodesic distance and then using, for example, Multidimensional Scaling to find points $y_i \in \mathbb{R}^d$ that minimize (say)

$$\min_{y_1,...,y_n \in \mathbb{R}^d} \sum_{i,j} \left(\|y_i - y_j\|^2 - \delta_{ij}^2 \right)^2,$$

which can be done with spectral methods (it is a good exercise to compute the optimal solution to the above optimization problem).

2.3 Semi-supervised learning

Classification is a central task in machine learning. In a supervised learning setting we are given many labelled examples and want to use them to infer the label of a new, unlabeled example. For simplicity, let's say that there are two labels, $\{-1, +1\}$.

Let's say we are given the task of labeling point "?" in Figure 10 given the labeled points. The natural label to give to the unlabeled point would be 1.

However, let's say that we are given not just one unlabeled point, but many, as in Figure 11; then it starts being apparent that -1 is a more reasonable guess.

Intuitively, the unlabeled data points allowed us to better learn the geometry of the dataset. That's the idea behind Semi-supervised learning, to make use of the fact that often one has access to many unlabeled data points in order to improve classification.
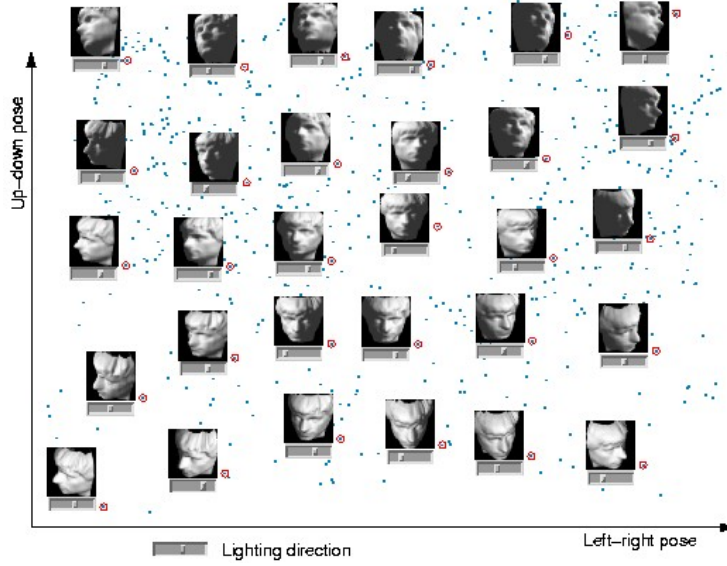
Figure 7: The two dimensional represention of a data set of images of faces as obtained in [TdSL00] using ISOMAP. Remarkably, the two dimensionals are interpretable

The approach we'll take is to use the data points to construct (via a kernel K_ε) a graph $G = (V, E, W)$ where nodes correspond to points. More precisely, let l denote the number of labeled points with labels $f_1, \ldots, f_l$, and u the number of unlabeled points (with $n = l + u$), the first l nodes $v_1, \ldots, v_l$ correspond to labeled points and the rest $v_{l+1}, \ldots, v_n$ are unlabaled. We want to find a function $f : V \to \{-1, 1\}$ that agrees on labeled points: $f(i) = f_i$ for $i = 1, \ldots, l$ and that is "as smooth as possible" the graph. A way to pose this is the following

$$\min_{f:V \to \{-1,1\}:\, f(i)=f_i\ i=1,\ldots,l} \sum_{i<j} w_{ij} \left(f(i) - f(j) \right)^2.$$

Instead of restricting ourselves to giving $\{-1, 1\}$ we allow ourselves to give real valued labels, with the intuition that we can "round" later by, e.g., assigning the sign of $f(i)$ to node i.

We thus are interested in solving

$$\min_{f:V \to \mathbb{R}:\, f(i)=f_i\ i=1,\ldots,l} \sum_{i<j} w_{ij} \left(f(i) - f(j) \right)^2.$$

If we denote by f the vector (in $\mathbb{R}^n$ with the function values) then we are can rewrite the problem
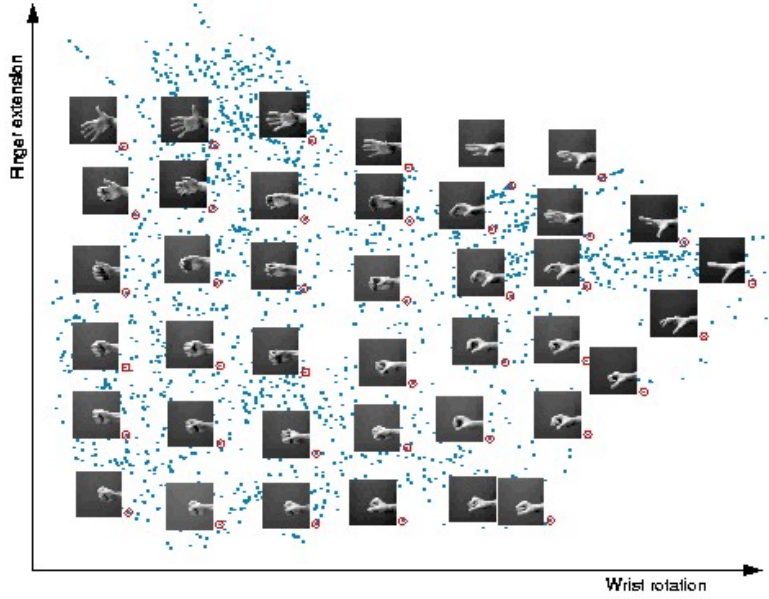
14

Figure 8: The two dimensional represention of a data set of images of human hand as obtained in [TdSL00] using ISOMAP. Remarkably, the two dimensionals are interpretable

as

$$
\begin{aligned}
\sum_{i<j} w_{ij}\left(f(i)-f(j)\right)^2 &= \sum_{i<j} w_{ij}\left[(e_i-e_j)\,f\right]\left[(e_i-e_j)\,f\right]^T \\
&= \sum_{i<j} w_{ij}\left[(e_i-e_j)^T\,f\right]^T\left[(e_i-e_j)^T\,f\right] \\
&= \sum_{i<j} w_{ij} f^T\left(e_i-e_j\right)\left(e_i-e_j\right)^T f \\
&= f^T\left[\sum_{i<j} w_{ij}\left(e_i-e_j\right)\left(e_i-e_j\right)^T\right] f
\end{aligned}
$$

The matrix $\sum_{i<j} w_{ij}\left(e_i-e_j\right)\left(e_i-e_j\right)^T$ will play a central role throughout this course, it is called the graph Laplacian [Chu97].

$$
L_G := \sum_{i<j} w_{ij}\left(e_i-e_j\right)\left(e_i-e_j\right)^T.
$$

Note that the entries of L_G are given by

$$
(L_G)_{ij} = \begin{cases} -w_{ij} & \text{if } i \neq j \\ \deg(i) & \text{if } i = j, \end{cases}
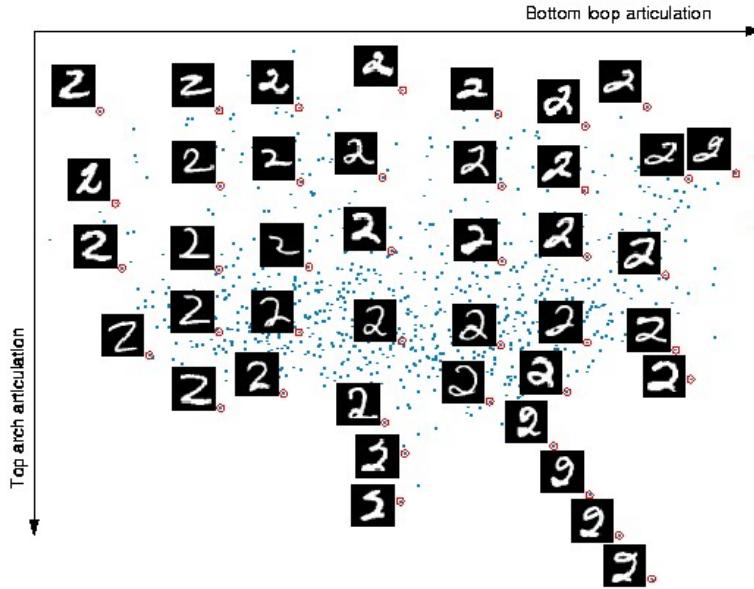$$

meaning that

$$
L_G = D - W,
$$

15

Figure 9: The two dimensional represention of a data set of handwritten digits as obtained in [TdSL00] using ISOMAP. Remarkably, the two dimensionals are interpretable
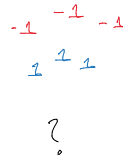

Figure 10: Given a few labeled points, the task is to label an unlabeled point.

where D is the diagonal matrix with entries $D_{ii} = \deg(i)$.

Remark 2.12 *Consider an analogous example on the real line, where one would want to minimize*

$$\int f'(x)^2 dx.$$

Integrating by parts

$$\int f'(x)^2 dx = \text{Boundary Terms} - \int f(x)f''(x)dx.$$

Analogously, in $\mathbb{R}^d$:

$$\int \|\nabla f(x)\|^2\, dx = \int \sum_{k=1}^{d} \left(\frac{\partial f}{\partial x_k}(x)\right)^2 dx = \text{B. T.} - \int f(x) \sum_{k=1}^{d} \frac{\partial^2 f}{\partial x_k^2}(x)dx = \text{B. T.} - \int f(x)\Delta f(x)dx,$$
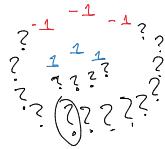
16

Figure 11: In this example we are given many unlabeled points, the unlabeled points help us learn the geometry of the data.

which helps motivate the use of the term graph Laplacian.

Let us consider our problem

$$\min_{f:V\to\mathbb{R}:\ f(i)=f_i\ i=1,\dots,l} f^T L_G f.$$

We can write

$$D = \begin{bmatrix} D_l & 0 \\ 0 & D_u \end{bmatrix}, \quad W = \begin{bmatrix} W_{ll} & W_{lu} \\ W_{ul} & W_{uu} \end{bmatrix}, \quad L_G = \begin{bmatrix} D_l - W_{ll} & -W_{lu} \\ -W_{ul} & D_u - W_{uu} \end{bmatrix}, \quad \text{and } f = \begin{bmatrix} f_l \\ f_u \end{bmatrix}.$$

Then we want to find (recall that $W_{ul} = W_{lu}$)

$$\min_{f_u \in \mathbb{R}^u} f_l^T \left[D_l - W_{ll} \right] f_l - 2 f_u^T W_{ul} f_l + f_u^T \left[D_u - W_{uu} \right] f_u.$$

by first-order optimality conditions, it is easy to see that the optimal satisfies

$$(D_u - W_{uu}) f_u = W_{ul} f_l.$$

If $D_u - W_u u$ is invertible[5] then

$$f_u^* = (D_u - W_{uu})^{-1} W_{ul} f_l.$$

Remark 2.13 *The function f function constructed is called a harmonic extension. Indeed, it shares properties with harmonic functions in euclidean space such as the mean value property and maximum principles; if v_i is an unlabeled point then*

$$f(i) = \left[D_u^{-1} \left(W_{ul} f_l + W_{uu} f_u \right) \right]_i = \frac{1}{\deg(i)} \sum_{j=1}^{n} w_{ij} f(j),$$

which immediately implies that the maximum and minimum value of f needs to be attained at a labeled point.

2.3.1 An interesting experience and the Sobolev Embedding Theorem

Let us try a simple experiment. Let's say we have a grid on $[-1,1]^d$ dimensions (with say m^d points for some large m) and we label the center as $+1$ and every node that is at distance larger or equal to 1 to the center, as -1. We are interested in understanding how the above algorithm will label the
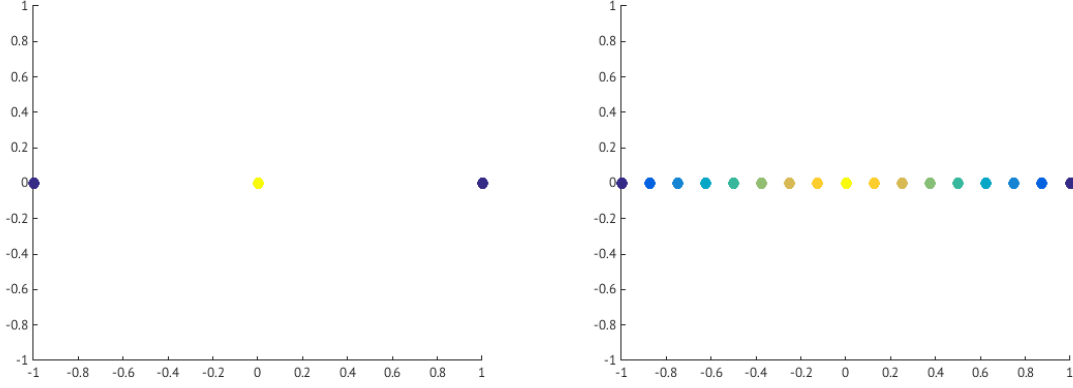
Figure 12: The $d = 1$ example of the use of this method to the example described above, the value of the nodes is given by color coding. For $d = 1$ it appears to smoothly interpolate between the labeled points.

remaining points, hoping that it will assign small numbers to points far away from the center (and close to the boundary of the labeled points) and large numbers to points close to the center.

See the results for $d = 1$ in Figure 12, $d = 2$ in Figure 13, and $d = 3$ in Figure 14. While for $d \leq 2$ it appears to be smoothly interpolating between the labels, for $d = 3$ it seems that the method simply learns essentially -1 on all points, thus not being very meaningful. Let us turn to $\mathbb{R}^d$ for intuition:

Let's say that we want to find a function in $\mathbb{R}^d$ that takes the value 1 at zero and -1 at the unit sphere, that minimizes $\int_{B_0(1)} \|\nabla f(x)\|^2 dx$. Let us consider the following function on $B_0(1)$ (the ball centered at 0 with unit radius)

$$f_\varepsilon(x) = \begin{cases} 1 - 2\frac{|x|}{\varepsilon} & \text{if} |x| \leq \varepsilon \\ -1 & \text{otherwise.} \end{cases}$$

A quick calculation suggest that

$$\int_{B_0(1)} \|\nabla f_\varepsilon(x)\|^2 dx = \int_{B_0(\varepsilon)} \frac{1}{\varepsilon^2} dx = \text{vol}(B_0(\varepsilon))\frac{1}{\varepsilon^2} dx \approx \varepsilon^{d-2},$$

meaning that, if $d > 2$, the performance of this function is improving as $\varepsilon \to 0$, explaining the results in Figure 14.

One way of thinking about what is going on is through the Sobolev Embedding Theorem. $H^m\left(\mathbb{R}^d\right)$ is the space of function whose derivatives up to order m are square-integrable in $\mathbb{R}^d$, Sobolev Embedding Theorem says that if $m > \frac{d}{2}$ then, if $f \in H^m\left(\mathbb{R}^d\right)$ then f must be continuous, which would rule out the behavior observed in Figure 14. It also suggests that if we are able to control also second derivates of f then this phenomenon should disappear (since $2 > \frac{3}{2}$). While we will not describe

---

[5]It is not difficult to see that unless the problem is in some form degenerate, such as the unlabeled part of the graph being disconnected from the labeled one, then this matrix will indeed be invertible.
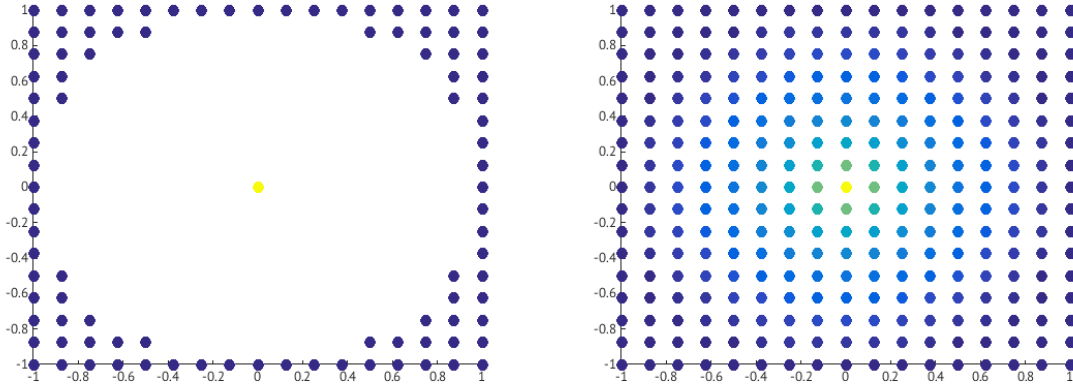
Figure 13: The $d = 2$ example of the use of this method to the example described above, the value of the nodes is given by color coding. For $d = 2$ it appears to smoothly interpolate between the labeled points.

it here in detail, there is, in fact, a way of doing this by minimizing not $f^T L f$ but $f^T L^2 f$ instead, Figure 15 shows the outcome of the same experiment with the $f^T L f$ replaced by $f^T L^2 f$ and confirms our intuition that the discontinuity issue should disappear (see, e.g., [NSZ09] for more on this phenomenon).

References

[Ban15]   A. S. Bandeira. Relax and Conquer BLOG: 18.S096 Graphs, Diffusion Maps, and Semi-supervised Learning. 2015.

[BR13]   Q. Berthet and P. Rigollet. Complexity theoretic lower bounds for sparse principal component detection. *Conference on Learning Theory (COLT)*, 2013.

[Chu97]   F. R. K. Chung. *Spectral Graph Theory*. AMS, 1997.

[Chu13]   M. Chudnovsky. The erdos-hajnal conjecture – a survey. 2013.

[Coh15]   G. Cohen. Two-source dispersers for polylogarithmic entropy and improved ramsey graphs. *Electronic Colloquium on Computational Complexity*, 2015.

[Con09]   David Conlon. A new upper bound for diagonal ramsey numbers. *Annals of Mathematics*, 2009.

[CZ15]   E. Chattopadhyay and D. Zuckerman. Explicit two-source extractors and resilient functions. *Electronic Colloquium on Computational Complexity*, 2015.

[DM13]   Y. Deshpande and A. Montanari. Finding hidden cliques of size $\sqrt{N/e}$ in nearly linear time. *Available online at arXiv:1304.7047 [math.PR]*, 2013.
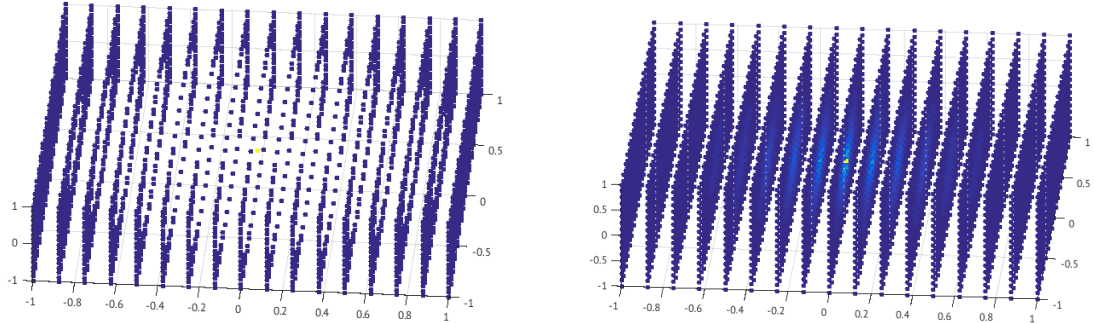
Figure 14: The $d = 3$ example of the use of this method to the example described above, the value of the nodes is given by color coding. For $d = 3$ the solution appears to only learn the label -1.
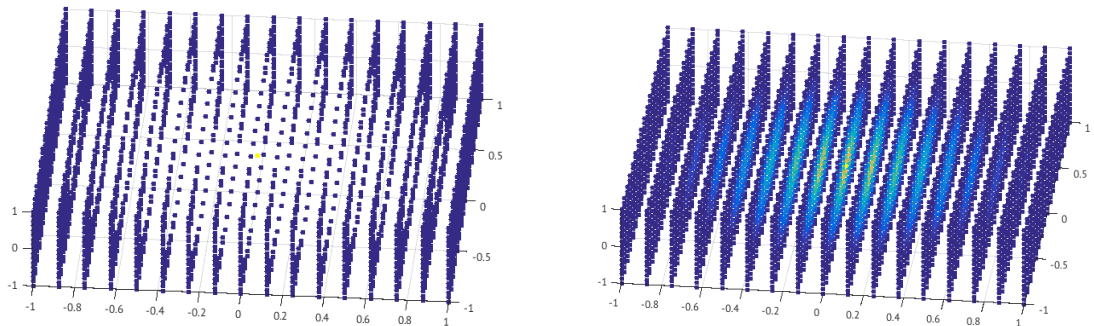

Figure 15: The $d = 3$ example of the use of this method with the extra regularization $f^T L^2 f$ to the example described above, the value of the nodes is given by color coding. The extra regularization seems to fix the issue of discontinuities.

[EH89]   P. Erdos and A. Hajnal. Ramsey-type theorems. *Discrete Applied Mathematics*, 25, 1989.

[NSZ09]   B. Nadler, N. Srebro, and X. Zhou. Semi-supervised learning with the graph laplacian: The limit of infinite unlabelled data. 2009.

[Ram28]   F. P. Ramsey. On a problem of formal logic. 1928.

[Spe75]   J. Spencer. Ramsey's theorem – a new lower bound. *J. Combin. Theory Ser. A*, 1975.

[Spe94]   J. Spencer. *Ten Lectures on the Probabilistic Method: Second Edition*. SIAM, 1994.

[TdSL00] J. B. Tenenbaum, V. de Silva, and J. C. Langford. A global geometric framework for nonlinear dimensionality reduction. *Science*, 290(5500):2319–2323, 2000.